Thomas Precession is the Basis for the Structure of Matter and Space

Einstein's theory of special relativity was incomplete as originally formulated since it did not include the rotational effect described twenty years later by Thomas, now referred to as Thomas precession. Though Thomas precession has been accepted for decades, its relationship to particle structure is a recent discovery, first described in an article titled "Electromagnetic effects and structure of particles due to special relativity". Thomas precession acts as a velocity dependent counter-rotation, so that at a rotation velocity of $\sqrt{3}/2\,c$, precession is equal to rotation, resulting in an inertial frame of reference. During the last year and a half significant progress was made in determining further details of the role of Thomas precession in particle structure, fundamental constants, and the galactic rotation velocity. In this article, these discoveries are described and proofs are provided, with results matching experimentally determined values to between eight and thirteen significant digits. Among the discoveries described and proven herein are 1) the observed galactic rotation velocity and elementary particle spin interact due to Thomas precession, 2) the basis for Planck's constant and quantized energy levels is Thomas precession, 3) the fine structure constant is a function of galactic rotation velocity and the maximum value of rotation velocity minus precession velocity. Also discovered and proven is that, due to the inertial frame of reference resulting from Thomas precession, distance and time, with units meters and seconds, within three dimensional space are sufficient to describe the structure of particles and their interactions. Einstein showed that energy is dependent on frame of reference with his equation $E = \gamma\, mc^2$, and he formulated $E = mc^2$ as rest energy. Proven herein is that particle mass and rest energy are functions of rotational velocity due to Thomas precession. These far reaching discoveries are all interrelated, and based in Thomas precession. The theory, models, and equations give results that match experimental data to very high precision.

Preston Guynn
Guynn Engineering, 1776 Heritage Center Drive, Suite 204
Wake Forest, North Carolina, United States 27587
guynnengineering@gmail.com

1. Introduction

Thomas precession and the discoveries presented herein follow from special relativity as it was developed by Albert Einstein. Einstein described his relativity principle as[1] "Every coordinate system that is in uniform translational motion relative to a justified system is again a justified system. The equations of motion of any system are the same with respect to all such justified systems." He also wrote that the special theory of relativity is arrived at by combining his relativity principle with[1] "the principle of the constancy of the velocity of light (Lorentz's theory)".

Relativistic length contraction and time dilation are consequences of these two principles. Einstein wrote[1] "Thus, by being set into motion, the body changes its shape to some extent, even though only for a reference system that does not take part in the body's motion. This change of shape consists in a

$$1 : \sqrt{1 - \frac{v^2}{c^2}}$$

contraction of all lengths in the direction of the motion." He followed this with the effect of relative motion on the rate of passage of time, and wrote "the clock moving with velocity v runs slower than it would run if it were at rest" followed by "this astounding consequence holds not only for clocks but also for the lapse of time of arbitrary processes."

Since length contraction occurs only in the direction of relative motion, angles are also relative to observer velocity. As an example, for an observer moving relative to a triangle, only the length of the triangle in the direction of observer motion is contracted. Figure 1 below depicts length and angle as functions of velocity for two velocities, where c is the speed of light.

length(v=0) = 1
length(v= $\frac{\sqrt{3}}{2}$ c) = 1

ϕ (v=0) = 0.463647609 radians
ϕ (v= $\frac{\sqrt{3}}{2}$ c) = 0.785398163 radians

length(v=0) = 2
length(v= $\frac{\sqrt{3}}{2}$ c) = 1

ϕ
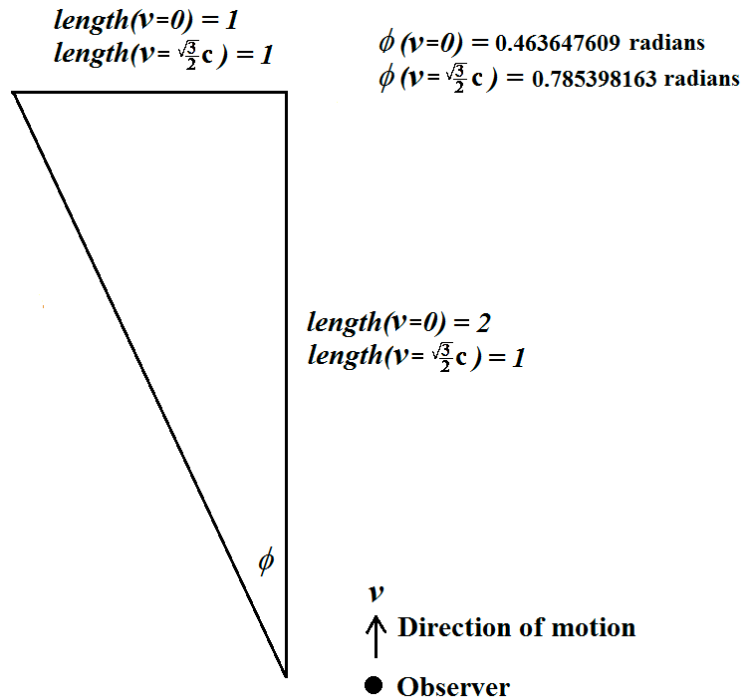
v

↑ **Direction of motion**

● **Observer**

Figure 1: Angles are velocity dependent

The velocity dependence of angles has an important effect with regard to rotational motion. Angular rotation is accompanied by angular precession, where precession has the sense of counter rotation. This is Thomas precession, as shown in Figure 2 below
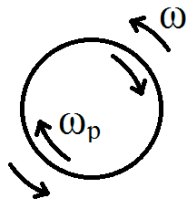

Figure 2: Angular rotation and angular precession

Nobel Laureate George Smoot provided a beautifully succinct equation for Thomas precession that applies to symmetrical rotation[2]

$$\frac{\omega_P}{\omega} = \frac{\Delta\theta}{2\pi} = \gamma - 1 \qquad \text{Smoot's equation} \qquad (1)$$

where ω is angular rotation, ω_p is angular precession, $\Delta\theta$ is the relativistic change in angle due to rotation, and γ is the Lorentz factor

$$\gamma \equiv \frac{1}{\sqrt{1-\left(\dfrac{v}{c}\right)^2}} \qquad (2)$$

where v is relative velocity, and c is the speed of light. Smoot's formulation is very helpful; it combines in a single expression 1) the relativistic fraction of a revolution as a function of the Lorentz transform, and 2) the relativistic

angular precession fraction of rotation as a function of the Lorentz transform. From Smoot's formulation it is readily apparent that the following proofs are based on Thomas precession.

2. Thomas precession describes limiting and unique characteristics

Since precession is in the opposite direction of rotation, Smoot's equation can be rearranged to define difference angular velocity, ω_d, as rotation angular velocity minus precession angular velocity

$$\omega_d = \omega - \omega_P = \omega(2 - \gamma) \qquad \text{Difference angular velocity equation} \qquad (3)$$

Difference angular velocity, ω_d, has great physical significance as the effective angular velocity with regard to angular momentum and kinetic energy. Multiplying both sides of the equation above by the radius at which the rotation occurs, the difference velocity can be formulated in terms of rotation velocity

$$v_d = v(2 - \gamma) \qquad \text{Difference velocity equation} \qquad (4)$$

With rotation velocity in one direction and precession velocity in the opposite direction, the difference velocity, v_d, represents the effective velocity. Difference velocity is graphed relative to rotation velocity in Figure 3.
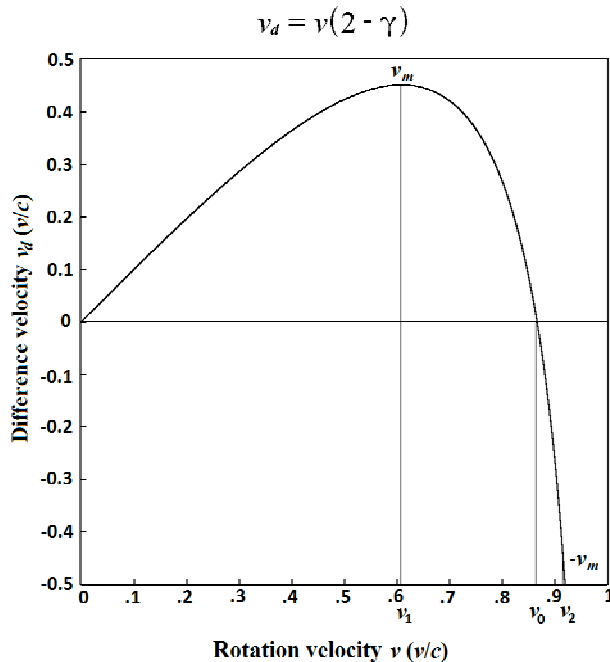

Figure 3: Difference velocity as a function of rotation velocity

The relationship between difference velocity and rotation velocity shown in Figure 3 is central to all that follows. Solving Equation 4 for the maximum difference velocity results in

$$v_m = (2^{2/3}-1)^{3/2} c \quad \approx 134965504.63776 \text{ m/s} \qquad (5)$$

The difference velocity equation is not constrained in terms of mass or dimensions. The relationship applies on all scales, from that of elementary particles to that of a galaxy. In a previous paper[3] it was proven that electrons are particles with rotation on three mutually orthogonal axes, always coupled to space, with difference velocity remaining between v_m and $-v_m$. Numerous additional discoveries proceeded from this structural model of the electron. For reference in the proofs that follow, designators are given to the rotation velocities of significance, and characteristics at those rotation velocities are listed in Table 1 below. The electron rotation velocity at which

$v_d = v_m$ is designated v_1. The electron rotation velocity at which $v_d = -v_m$ is designated v_2, and the rotation velocity at which $v_d = 0$, between v_1 and v_2, is designated v_0. These designators are shown in Figure 3 above. Characteristics at the three annotated rotation velocities, relative to the laboratory frame of reference, are

Characteristics at rotation velocity v_1	
v/c	$v_1/c \approx 0.6083087004577$
v(m/s)	$v_1 \approx 182366360.53300$
v_d	v_m
γ	$\gamma_1 = \sqrt[3]{2} \approx 1.2599210498949$
$\Delta\theta$ (rad)	$\Delta\theta_1 \approx 1.6331321217262$

Characteristics at rotation velocity v_0	
v/c	$v_0/c = \sqrt{3}/2 \approx 0.8660254037844$
v(m/s)	$v_0 \approx 259627884.49098$
v_d	0.0 m/s
γ	$\gamma_0 = 2.0$
$\Delta\theta$ (rad)	$\Delta\theta_0 = 2\pi \approx 6.28318530717959$

Characteristics at rotation velocity v_2	
v/c	$v_2/c \approx 0.9159200289968$
v(m/s)	$v_2 \approx 274585916.82437$
v_d	$-v_m$
γ	$\gamma_2 = 2.49152376858454$
$\Delta\theta$ (rad)	$\Delta\theta_2 \approx 9.37152022807954$

Table 1: Characteristics at designated rotation velocities

In Table 1, $\Delta\theta$ is calculated using Smoot's equation. The other values are components of solutions to the difference velocity equation. Some other characteristics particularly noteworthy are

$$2\left(\frac{v_1}{c}\right)^2 = (2 - \gamma_1) \tag{6}$$

and

$$\frac{\gamma_1^2}{2} = \frac{1}{\gamma_1} \tag{7}$$

In Equation 5, v_m was given as the analytical solution for the maximum value of v_d. Another representation of that solution is

$$v_m = \sqrt{3}(\gamma_1 - 1)c \tag{8}$$

A unique property of rotational motion described by the difference velocity equation and shown in Figure 3 is that $v_d = 0$ at rotation velocity $v = v_0$. Since precession is in the opposite direction of rotation, and is equal in magnitude, they cancel, and there is effectively no rotation velocity at v_0. This unique property at v_0, which follows directly from Thomas precession, characterizes an inertial frame of reference. Though Einstein's description of a "justified system", which today is referred to as an inertial frame of reference, incorporated uniform translational motion, the characteristics of rotation at v_0 meet the operational definition of a justified system. There is no net acceleration, angular momentum, or kinetic energy at v_0 relative to the lab frame of reference.

Another unique property of rotational motion at v_0 is that $\varDelta\theta_0 = 2\pi$. As shall be shown, the 2π difference in angle between the lab frame of reference and the rotating inertial frame of reference at v_0 results in angular scaling between the two frames.

Some significant characteristics of rotation have been detailed for reference throughout the following, and it has been stated that electron rotation is on three axes with rotation velocity bounded by velocities designated v_1 and v_2 in Figure 3. The proof of this statement relates to experimentally determined characteristics of electron, proton, and photon, so experimentally determined characteristics are listed below.

Experimentally determined electron and proton characteristics	
Per-axis angular momentum $\mathbf{S_z}$	$\pm \hbar/2$
Total angular momentum $\mathbf{S}$	$\pm\left(\sqrt{3}/2\right)\hbar$

Experimentally determined photon characteristics	
On-axis angular momentum	$\hbar$
Total angular momentum	$\pm\sqrt{2}\hbar$
Energy	$\hbar\omega$

Table 2: Experimentally determined particle characteristics

Planck's constant is represented by h, and in Table 2, $\hbar$ is the reduced Planck constant, $h/(2\pi)$. Photon radian frequency is ω.

3. Electron structure and dynamics

It is necessary to provide details of electron structure and dynamics from previous work as a basis for the latest discoveries and proofs. Following is a description of the correspondence between Thomas precession and the electron's experimentally determined total and per-axis characteristics within the model discussed herein. As previously stated, electrons are particles with rotation on three mutually orthogonal axes, always coupled to space, with difference velocity remaining between v_m and $-v_m$. When electron rotation velocity on an axis is in the range v_1 to v_0, the electron angular momentum on that axis is positive, and when the rotation is in the range v_0 to v_2, the angular momentum is negative. This is because for the electron $S_z = R_e m_e/3\ v_d$, where S_z is the per axis magnitude of angular momentum, R_e is the electron radius, v_d is the difference velocity, and m_e is electron mass. Since v_d is positive in the range v_1 to v_0, S_z is positive in that range, and since v_d is negative in the range v_0 to v_2, S_z is negative in that range. At rotation velocity v_1, where $v_d = v_m$, $S_z = \hbar/2$, and at v_2, where $v_d = -v_m$, $S_z = -\hbar/2$. This is shown below in Figure 4.
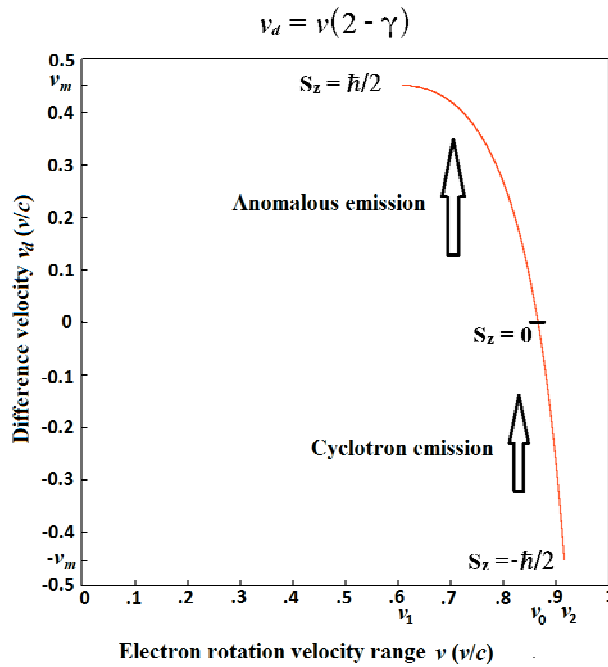
$$v_a = v(2 - \gamma)$$

Figure 4: Electron ring difference velocity as a function of rotation velocity, with angular momentum and emission range annotated.

When energy of photons emitted by an electron moving through a magnetic field is ascribed to magnetic moment, the magnetic moment vector points in the opposite direction of the electron's angular momentum vector. The proton magnetic moment and angular momentum vectors both point in the same direction, so by convention the proton magnetic moment is assigned a positive sign and electron magnetic moment is assigned a negative sign. The maximum total energy emitted by an electron in a magnetic field is when a cyclotron emission is followed by a "spin-flip" and emission of the "anomalous" photon[4]. Thus the sequential emissions, coinciding with a reversal of angular momentum, are associated with magnetic moment. The energy of the electron anomalous emission is much less than its cyclotron emission, but the sum of the two energies divided by two is the basis of magnetic moment of the electron. The rotation velocity range v_2 to v_0 is hereafter referred to as the Electron Cyclotron Range, and rotation velocity range v_0 to v_1 is referred to as the Electron Anomalous Range.

Note that the direction of rotation from v_1 to v_2 is the same, and yet the angular momentum, as a function of difference velocity, reverses. An understanding of this is very important, and Figure 5 below is to emphasize and clarify the point. Note in the One Loop Top View that the direction of rotation does not reverse, but in the One Loop Side View the direction of angular momentum reverses. With three mutually orthogonal loops, the total angular momentum vector can point in any direction, without the direction of rotation of the three loops changing.
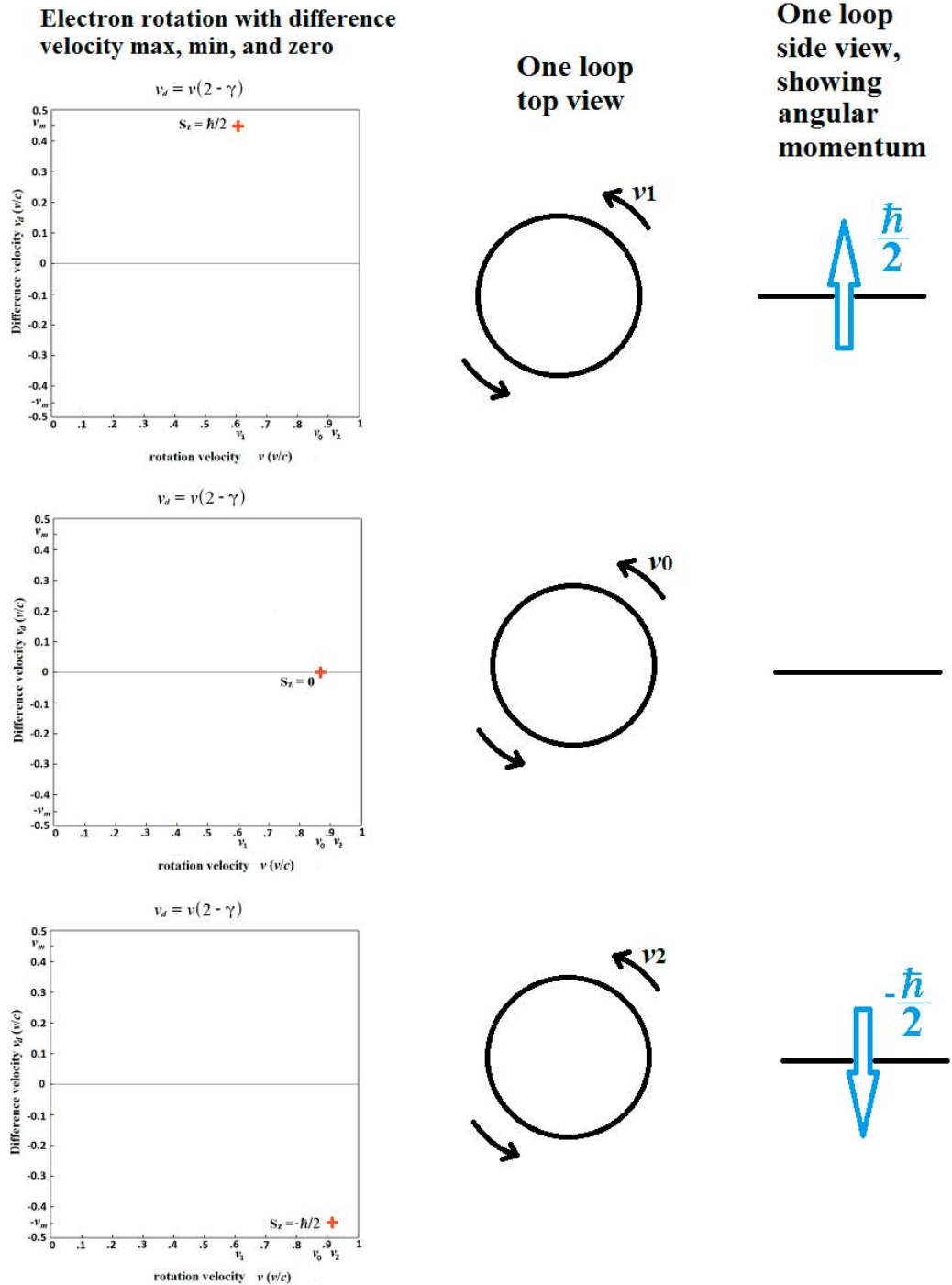
6

Figure 5: Electron single axis difference velocity, rotation velocity, and angular momentum

Figure 6, below, shows conditions for charges to emit a photon. It is emphasized that electrons and protons are always coupled to space, and photon emission is not an isolated event, but part of a continuing interaction between charged particles and space wherein angular momentum is always conserved.
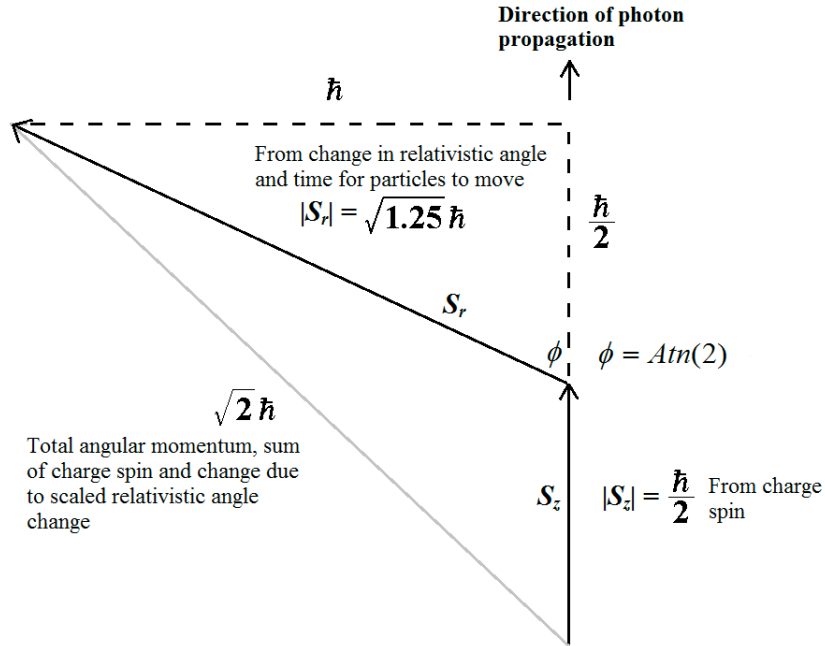
Figure 6: Conditions for photon emission

Photon emission is accompanied by a decrease in electron angular momentum on one axis of $\hbar/2$, as rotation velocity changes from v_2 to v_0, or v_0 to v_1. The change in angular momentum can be viewed as a transfer of angular momentum from the electron to the photon. However, photons have on-axis angular momentum of $\hbar$, and total angular momentum of $\pm\sqrt{2}\hbar$. The angular momentum vector that must be combined with the change in electron per axis angular momentum to realize both the on-axis and total angular momentum components of a photon is shown in the diagram above and is designated S_r.

The magnitude of S_r is $\sqrt{1.25}$ and the vector is at an angle $=$ Arctan(2) with respect to the on-axis electron angular momentum. This additional angular momentum vector is from the change in angle associated with the change in rotation velocity during photon emission, and the time over which an electron and proton move closer together.

3.1 High energy scattering is not an indicator of electron size

The statement has been made[5] that "High energy scattering from electrons shows no 'size' of the electron down to a resolution of about 10^{-3} fermis", and a commonly asked question when electron structure is presented is "why have experiments been unable to determine electron dimensions?" The answer is seen in the structure and dynamics described above. Once again referring to Figure 4, photon emission occurs when electron rotation velocity changes from v_2 to v_0, or v_0 to v_1. The combined on-axis transfer of angular momentum and relativistic change in angle, with particle movement, result in a photon with on-axis angular momentum of $\hbar$ and total angular momentum of $\pm\sqrt{2}\hbar$. Thus the emitted photon energy, wavelength, and frequency are not indicators of the electron's dimensions. For example, a transition from v_2 to v_0 takes some time, T. The energy of the emitted photon is $\hbar / T$. The energy, frequency, and wavelength of the photon exchange does not reveal the electron's dimensions. However, the electron radius can be determined from the available combined experimental data as described below.

4. A proof of electron and proton structure leads to latest discoveries

In an article titled *'Electrostatic Force and Charge Structure'*, the magnitude of the electrostatic force between two charged particles separated by distance r was formulated as[6]

$$F(r) = \frac{2\pi}{r^2 c} \left(\frac{\frac{\sqrt{3}}{2} \hbar k_1}{\frac{1}{2} m_e v_m^2} + \sqrt{2} \hbar v_m k_2 \right) \tag{9}$$

where

$$k_1 \equiv \text{kg m}^4/\text{s}^4 \tag{10}$$
$$k_2 \equiv \text{m/s} \tag{11}$$

and m_e is electron mass. Note that k_1 and k_2 effect unit transformations, changing the units but not changing the magnitude. Unit transformations, due to Thomas precession, are described in following sections. The first term in parentheses is charge total angular momentum divided by the kinetic energy of electron mass moving at v_m, with a change of units. The second term in parenthesis is photon total angular momentum multiplied by v_m, with a change of units. The 2π factor is $\Delta\theta_0$, due to the change in angle between the lab frame of reference and frame of reference at v_0. Both the angular momentum and kinetic energy in the first term, are consistent with a change in rotation velocity from v_2 to v_0, or v_0 to v_1. Values calculated using Equation 9 match the result of Coulomb's law applied to two elementary charges exactly. Equation 9 can be generalized to the force between charges q_1 and q_2 by multiplying on the right by the product of n_1 and n_2, where n_1 and n_2 are the number of charged particles at each location separated by distance r, between which the force is measured, with n_1 and n_2 taking the sign of the associated charge. Because the physical basis of electrostatic charge was previously unknown, an arbitrary system was developed based on the force between current carrying conductors separated by a distance of 1m. This defined current, and current for a period of one second defined charge. Equation 9 shows the electrostatic force in terms of particle structure due to Thomas precession, and particle dynamics. The units Coulomb and Ampere are no longer necessary to define or describe the force and potential energy between charged particles.

Because Equation 9 applies to both electrons and protons, the formulation reveals details of both electron and proton structure. This equation coupled with the experimentally determined per-axis and total angular momentum of proton and electron lead to the electron radius

$$R_e = \frac{\frac{\hbar}{2}}{\frac{m_e}{3} v_m} \approx 1.28663582937643\text{E} - 12 \text{ m} \tag{12}$$

and the proton maximum difference velocity

$$v_{mp} = v_m \sqrt{\frac{m_e}{m_p}} \cong 3149694.18144 \text{ m/s} \tag{13}$$

where m_p is proton mass. The proton radius is

$$R_p = \frac{\frac{\hbar}{2}}{\frac{m_p}{3} v_{mp}} \approx 3.00262603862771\text{E} - 14 \text{ m} \tag{14}$$

Confirming that these results match the experimentally determined values, the kinetic energy of one of an electron's three mutually orthogonal rings when rotating at v_m is

$$E_k = \frac{1}{2}\frac{m_e}{3}v_m^2 \cong 2.7655614\text{E-}15 \text{ J}$$ (15)

The kinetic energy of one of a proton's three mutually orthogonal rings when rotating at v_{mp} is

$$E_k = \frac{1}{2}\frac{m_p}{3}v_{mp}^2 \cong 2.7655614\text{E-}15 \text{ J}$$ (16)

Equations 15 and 16 show that the effective kinetic energy of electron and proton rings is equal when they are rotating with their difference velocities each at maximum. In addition the two particles have equivalent maximum difference angular velocities. For the electron,

$$\omega_m = v_m/R_e \cong 1.048979839953\text{E+}20$$ (17)

and for the proton,

$$\omega_m = v_{mp}/R_p \cong 1.048979839953\text{E+}20$$ (18)

With their maximum difference velocities, v_m and v_{mp}, and their calculated radii, R_e and R_p, electron and proton on-axis and total angular momentum match experimentally determined values. Moreover, the three axes total effective kinetic energies are equal, and they match the value in the denominator of the first parenthetical term in Equation 9. Furthermore, the difference angular velocities are equal to each other and are a valid solution of the difference angular velocity equation, Equation 3. In a previous article[3] proof of the radii was further validated through the neutron structure and mass, though that will not be repeated here.

The proton rings' difference velocity remains between +/- v_{mp}, with each ring's angular momentum S_Z = +/- ℏ/2 at +/- v_{mp}. This is shown in Figure 7 below.

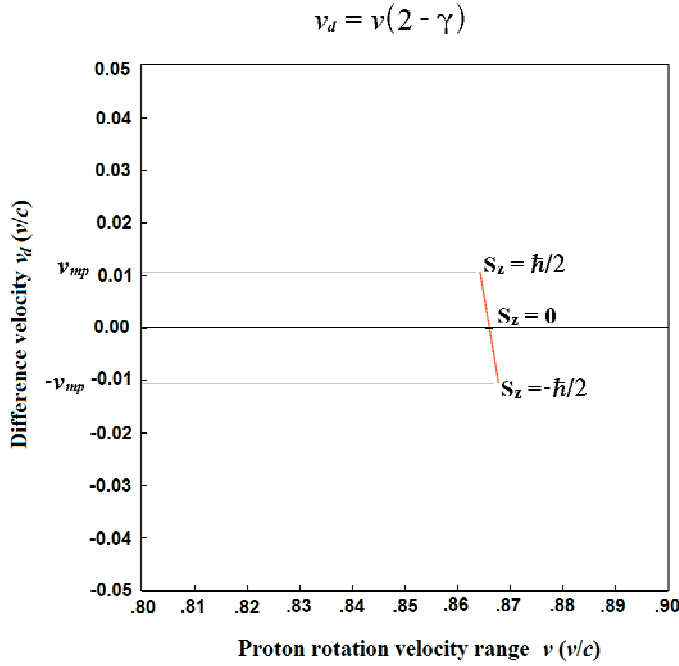$$v_d = v(2 - \gamma)$$

**Figure 7: Proton ring difference velocity as a function
of rotation velocity, with angular momentum annotated.**

The models of electron and proton given above have been shown to match their experimentally determined characteristics of per-axis and total angular momentum, and the electrostatic force has been formulated in terms of particle structure and dynamics with the result matching Coulomb's law applied to two elementary charges to eleven significant digits. The model explains how proton and electron, with very different masses, have the same angular momentum and the same magnitude of electrostatic force. It also provides the mechanism for spin-flip and for cyclotron and anomalous emissions to contribute to magnetic moment. Further, the very different shapes of electron and proton difference velocity curves gives the basis for their very different g factors.

Since Equation 9 for electrostatic force is related to the fine structure constant, the fine structure constant can be determined

$$\alpha = 2\pi \left(\frac{\sqrt{3}k_1}{v_m^2 m_e c^2} + \frac{\sqrt{2}v_m k_2}{c^2} \right) \qquad \text{Fine Structure Constant, Form A} \qquad (19)$$

The result of this equation matches the CODATA recommended value[7] to eleven significant digits.

Equation 9 for the magnitude of electrostatic force between two charged particles is consistent with the structural models of electrons and protons based on Thomas precession. The relationships between the terms are consistent with the dynamics described for the models. The models are directly related to Thomas precession.

The entirety of previous articles will not be repeated here, but proton and electron structure, the electrostatic force, and the fine structure constant are included to provide background for the latest discoveries. The previous discoveries also introduced unit transformations which are due to Thomas precession and the inertial frame of reference at v_0.

Previously, the theoretical basis given the for unit transformations in Equations 9 and 19 was the difference in angle between the lab frame of reference, and the inertial frame of reference at v_0. The difference in angle and the

11

asymmetry of time dilation, which occurs only in the direction of motion, justified the transformation of units. That justification is valid, but there are additional discoveries that validate unit transformations. The new discoveries lead to proofs that three spatial dimensions, distance, and time are sufficient to describe the characteristics previously described by units of mass, energy, and force. Distance per unit time is velocity, and the dependence of length and angle on velocity result in structure as shown in the following.

5. Special relativity, acceleration, and units of measure

After special relativity was introduced, a question was posed about time dilation, called the Twin Paradox. According to relativity theory, time dilation occurs with relative velocity. If twin siblings are in the same location and stationary, and then move relative to each other for a period of time, and then come back together and are stationary, how much of the time dilation that occured due to relative velocity will have applied to each? Should the twins have aged equally, or should one have aged more than the other? Since the paradox neglects both the directional asymmetry of time dilation and Thomas precession, statements concerning it are oversimplified. In general, the solution depends on how the twins interact with their initial frame of reference throughout the time of separation. At least one of the twins must accelerate or there is no movement and no paradox. Acceleration, which was outside the domain of special relativity, can be approached by bringing it into special relativistic terms.

A transition from one velocity to another velocity is defined as acceleration. Transitioning from rotation velocity v_1 to v_0 requires traversing every velocity in between, and in relativistic terms that is traversing every frame of reference in between. Since the same physics applies at each of these in-between velocities, the total relativistic effect of transitioning from v_1 to v_0 involves the integral of the Lorentz factor between the two velocities. As described in previous work[8], $c = 299792458$ m/s is a definition, not an experimental result, so in physical terms only the ratio v/c is significant. If c is redefined to another numerical value, the special relativistic physical effects at v/c remain the same. Treating the ratio v/c as the variable of integration, the Lorentz transform can be integrated.

$$\theta \equiv \int \frac{1}{\sqrt{1-(v/c)^2}} \, d\left(\frac{v}{c}\right) = \sin^{-1}\left(\frac{v}{c}\right) + C \tag{20}$$

The integral of the Lorentz transform is an angle. This is very significant because the Lorentz transform itself is unit-less. The effect of acceleration, a change of velocities, is an angle whose sine is v/c. This characteristic is consistent with the angular effects of Thomas precession. That an angle is the result of a change in velocities is another basic justification for the transformation of units due to relativistic effects. Application to physical structure is shown in the following sections.

Another basic justification for transformation of units due to Thomas precession is that the sine of an angle is

$$\sin\theta = \frac{v}{c} = \theta - \frac{\theta^3}{3!} + \frac{\theta^5}{5!} - \frac{\theta^7}{7!} + \dots \tag{21}$$

The relationship between the ratio v/c and the integral of the ratio's Lorentz transform involves not only an angle, but also the angle to an infinite number of odd powers. Inextricably related is the cosine of the angle

$$\cos\theta = \frac{1}{\gamma} = 1 - \frac{\theta^2}{2!} + \frac{\theta^4}{4!} - \frac{\theta^6}{6!} + \dots \tag{22}$$

The inverse of the Lorentz factor is the cosine of the angle which is the integral of the Lorentz factor, and it is also related to the angle to an infinite number of even powers. Below is a graphical representation of the relationship between $1/\gamma$, v/c, and θ.
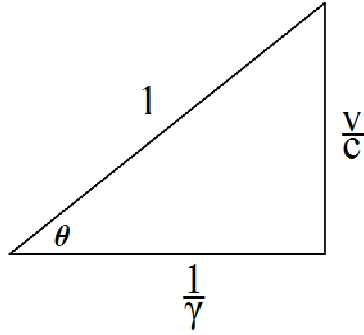
Figure 8: Relationship between velocity fraction of c, inverse of Lorentz transform, and integral of Lorentz transform

The physical application of these relationships to acceleration, or transition between velocities, is additional justification for transformation of units due to special relativistic Thomas precession. Application to physical structure is proven in the following sections. Figure 9 below is a graphical representation of the integral of the Lorentz transform with respect to v/c from v_1/c to v_0/c, the significance of which is detailed in following sections.
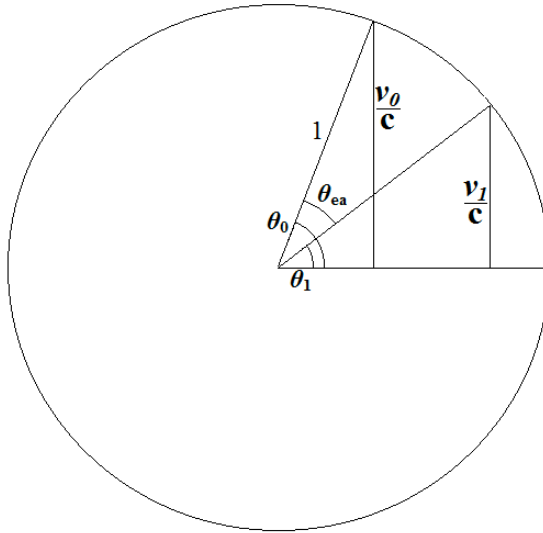

Figure 9: Graphical representation of integral of Lorentz transform over the electron anomalous range

The integral of the Lorentz transform with respect to v/c from v_1/c to v_0/c is,

$$\theta_{ea} \equiv \int_{v_1/c}^{v_0/c} \frac{1}{\sqrt{1-\left(\dfrac{v}{c}\right)^2}} \, d\left(\frac{v}{c}\right) \approx 0.39326960869637 \tag{23}$$

The "ea" subscript to θ refers to "electron anomalous", consistent with the rotation velocity designators and ranges previously described and shown in Figure 4. An angle as the integral of the Lorentz transform has a limit. Over the range $v/c = 0$ to $v/c = 1$, the Lorentz integral angular limit is

$$\theta_{L\max} \equiv \int_0^1 \frac{1}{\sqrt{1-x^2}} \, dx = \frac{\pi}{2} \tag{24}$$

13

This angular limit is another basic characteristic of space and time. The limit is an upper bound on an angular effect of transitioning velocity, analogous to c as an upper bound on velocity. Another Lorentz integral angle of significance is that from the non-rotating frame to the frame at v_0.

$$\theta_{L0} \equiv \int_0^{v_0/c} \frac{1}{\sqrt{1-x^2}} \, dx = \frac{\pi}{3} \tag{25}$$

Equation 9 for electrostatic force consists of two terms, the first showing some of the dynamics of change in rotation velocity, and the second independent of the change in velocity but related to the ratio of v_m to c^2. The integrals of the Lorentz factor over the change in rotation velocity are not apparent in that formulation, but they are related to the kinetic energy term, and indirectly to h. Equation 9 shows two different spatial, structural, and dynamical effects that combine to appear, with additional base units of mass and energy, as the derived unit of force. In the following it is shown that in three dimensional space, the base units of time and distance, with their derived units are not only sufficient to describe the effects labeled mass and energy, but actually give more insights to the physics of structures and their interactions.

Essential to proofs that special relativistic Thomas precession is the basis for structure, from the scale of elementary particles to the scale of galaxies, is the maximum galactic rotation velocity.

6. Milky Way Maximum Galactic Rotation Velocity

Star systems of spiral galaxies rotate around their galactic centers at velocities that increase with radial distance up to a limiting velocity, beyond which their velocities do not match predictions based on gravitational theory[9]. A hypotheses given to explain the divergence was "dark matter". However, because Thomas precession is expected to affect rotation velocities, and because Thomas precession is not limited by scale or mass, in previous work the hypotheses was proposed that maximum galactic rotation velocities are due to Thomas precession[3]. The hypothesis is proven in the following.

Relevant to the proof is that our solar system lies beyond the radial distance from the center of the Milky Way at which star system velocities begin being limited. The International Astronomical Union recommends 220000 m/s as the galactic rotation velocity at the distance of the solar system from the center of the Milky Way[10]. A recent study by de Gris and Bono concludes that "there is no compelling evidence that the IAU-recommended $\theta_0 = 220$ km s^{-1} is no longer valid". In IAU usage, θ_0 is the rotation velocity of the solar system around the galactic center, not to be confused with θ_0 used elsewhere in this article. de Gris and Bono suggest increasing the value to 225 km s^{-1} only if the recommended galactocentric distance is reduced. The IAU value and that of deGris and Bono bracket the magnitude of the value determined based on Thomas precession. Based on calculations that follow, the observed galactic rotation velocity at the solar system is more precisely

$$v_g = -221677.92498 \text{ m/s} \tag{26}$$

The observed velocity is a difference velocity due to Thomas precession. The minus sign indicates that the solar system's galactic precession velocity exceeds rotation velocity. The observed velocity as a function of the rotation velocity is shown in the difference velocity graph of Figure 10 below.
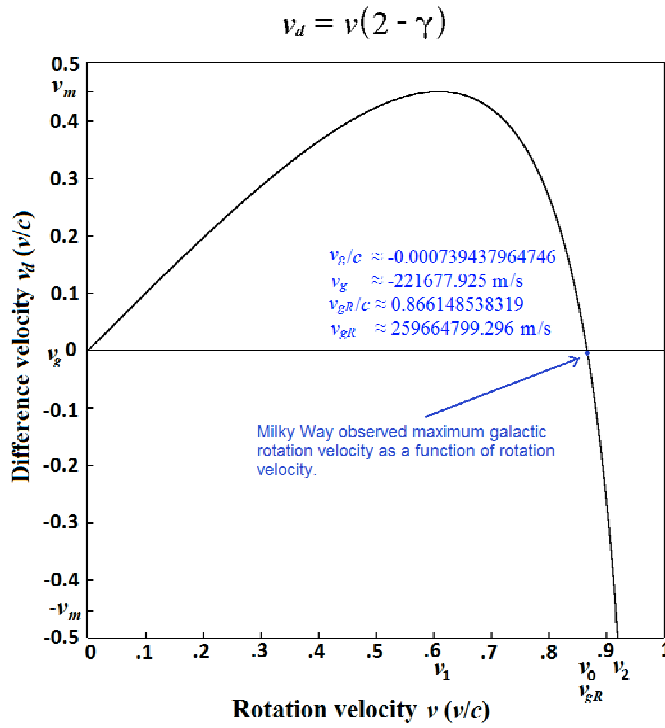
Figure 10: Galactic difference velocity v_g as a function of rotation velocity v_{gR}

Because the solar system is in a region where the observed galactic rotation velocity is at a limit, it was expected that the limit was related to or interacted with the relativistic rotational properties of elementary particles in the region. That is, rotation of particles according to Thomas precession as shown in previous sections interacts with difference velocity v_g and rotation velocity v_{gR}. Examples of this are shown in the following sections. It should be briefly mentioned that there are several relevant inertial frames of reference. The origin of the graph above is at the non-rotating inertial frame of reference at the galactic center, with respect to which the solar system is rotating at v_{gR}. There is also an inertial frame of reference with respect to which astronomers measure v_g, which is at rotation velocity v_0. Elementary particles rotating as shown in previous sections have an inertial frame of reference at v_0. As a reminder, a frame of reference in special relativity describes not a location but a velocity.

6.1 Derivation of v_g through the electron cyclotron rotation range

Based on the theory previously described, two interrelated equations can be formulated. The simultaneous solution to the two equations gives v_g. The first equation gives a very slight adjustment to v_2 / c that applies to particle rotation measured here in the solar system, due to v_g. The adjustment is only one part in 10^9. The second equation gives v_g in terms of the integral of the Lorentz transform over the adjusted electron cyclotron rotation range.

$$\frac{v_2'}{c} = \frac{v_2}{c}\left(1 - \frac{(\gamma_1 - 1)k_2}{c - \frac{v_g}{\sqrt{3}}}\right) \tag{27}$$

$$\frac{v_2'}{c} \approx 0.91592002820299 \tag{28}$$

15

$$\theta_{ec} = \int_{\frac{v_0}{c}}^{\frac{v_2'}{c}} \frac{1}{\sqrt{1-(v/c)^2}} \, d\left(\frac{v}{c}\right) \approx 0.11059667926806 \tag{29}$$

$$\frac{v_g}{c} = \frac{1}{\pi}\left(1 - \frac{1}{3\sqrt{\theta_{ec}}}\right) \approx -7.39437964740\text{E} - 04 \tag{30}$$

$$v_g \approx -221677.924988 \text{ m/s} \tag{31}$$

The unprimed v_2, as shown in Figure 4, is simply the rotation velocity for which Equation 4 results in $v_d = -v_m$, while v_2' is v_2 adjusted for the particle frame of reference. The two interrelated equations give a single result for v_g /c which will be shown to be accurate to eleven significant digits. The equation adjusting the electron rotation velocity range scales that velocity range, an extremely small amount, from the particle's inertial frame of reference to the laboratory frame of reference, where our difference velocity is v_g. Without the adjustment to the electron cyclotron range, Equation 30 would give v_g /c with six significant digits of accuracy. Because of the slope of the Lorentz transform at v_2, the tiny adjustment that results in v_2' improves the accuracy by an additional five significant digits. The unit conversion factor k_2 in Equation 27 is consistent with the previous usage. The "ec" subscript to θ refers to "electron cyclotron". The relationship between particle rotation and galactic rotation can be depicted graphically
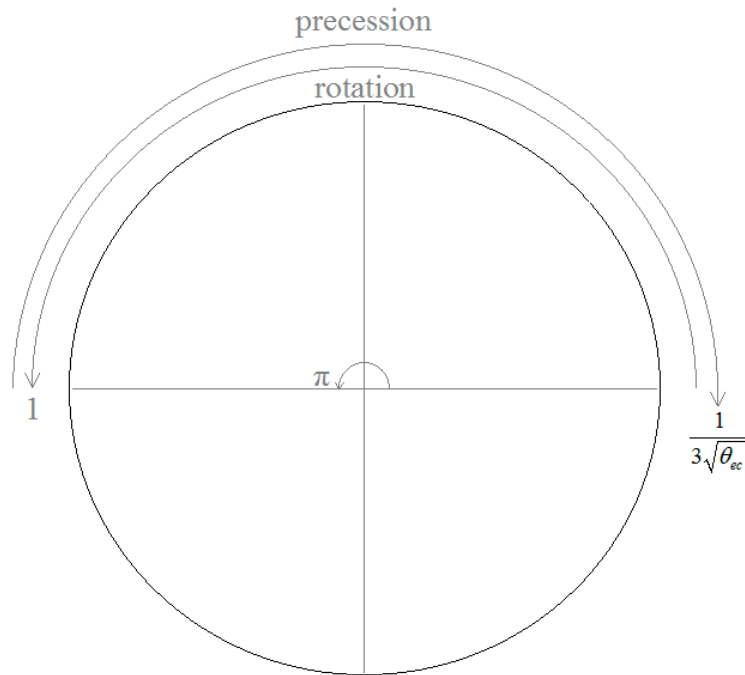

Figure 11: Graphical representation of relationship between particle rotation and galactic rotation

The observed maximum galactic rotation velocity, v_g, has an extremely important role in all of physics.

6.2 The Fine Structure constant, *α*, as a function of *v_g*

In Equation 19, Form A of the fine structure constant was formulated in terms including m_e. There is a more basic relationship in terms of $|v_g|$.

$$\alpha = 2\pi \left(\frac{|v_g|}{\sqrt{2}v_m} + \frac{\sqrt{2}v_m k_2}{c^2} \right) \qquad \text{Fine Structure Constant, Form B} \qquad (32)$$

The value calculated for *α* using Equation 32 matches the CODATA recommended value to eleven significant digits[7]. The calculation using only the first of the two parenthetical terms would match six significant digits. The electrostatic force can be formulated in terms of *α*, giving further insights from Thomas precession. A general equation for the electrostatic force between charges separated by distance *r* is

$$F(r) = \left(\frac{|v_g|}{\sqrt{2}v_m} + \frac{\sqrt{2}v_m k_2}{c^2} \right) \frac{hc}{r^2} n_a n_b \qquad \text{Analog to Coulomb's law} \qquad (33)$$

where n_a and n_b are the number of charged particles at each location separated by distance *r*, and n_a and n_b also carry the sign of the charge. The parenthetical quantity is $\alpha / (2\pi)$, and is unit-less. The factor following the parentheses has units of force. Considering the effect of Thomas precession on electrostatic force, the first term in parentheses is the ratio of difference velocities. The denominator of the first term is the magnitude of the vector sum of v_m on two axes. The electrostatic force is approximately proportional to the ratio of the magnitude of the difference velocity, $|v_g|$, to the maximum difference velocity v_m. In the fine structure constant Form A of Equation 19, the first parenthetical term required unit transformation k_1. However, in the formulation of Form B, k_1 is not required.

6.3 Electron mass and rest energy as functions of *v_g*

Einstein proposed the concept of rest energy as part of his theory of special relativity. His derivation started with[1] "an electrically charged point mass", and restricted the development to linear motion. After deriving an equation equivalent to $E = \gamma mc^2$, he expanded it to $E = mc^2 + 1/2\ mv^2 + ...$. He commented that the second term of the expansion is the familiar term for kinetic energy and rhetorically asked what the first velocity independent term signified. Because the two terms are part of the same expansion, he wrote[1] "One is therefore already inclined at this point to grant a real significance to this term mc^2, to view it as the expression for the energy of the point at rest."

Because charge spin was not known at the time, Einstein viewed a stationary charge as "at rest". Building on Einstein's and Thomas' work, and that of researchers who determined galactic rotation and charge spin, the "rest" energy of the electron can now be formulated as

$$E = m_e c^2 = \frac{\sqrt{2}\sqrt{3}k_1}{|v_g|v_m} \qquad (34)$$

The mass of the electron can then be expressed as

$$m_e = \frac{\sqrt{2}\sqrt{3}k_1}{|v_g|v_m c^2} \qquad (35)$$

The experimentally determined value of the electron mass is given by CODATA to nine significant digits, and the result of Equation 35 matches the CODATA recommended value exactly[7]. The expression for electron mass reveals that the measurement is actually a measure proportional to the inverse of the product $v_g\, v_m\, c^2$. Particles in every laboratory on earth are rotating around the galactic center at a velocity, v_{gR}, for which precession exceeds rotation by an average of v_g. Electrons rotate in three dimensions about their own axes, with change in rotation affected by their frame of reference.

7. Proton/Electron mass ratio

In Equations 27-30, the electron cyclotron range was shown to be modified by one part in 10^9 by v_g, and v_g was shown to be a function of the integral of the Lorentz transform over the electron cyclotron range. The proton/electron mass ratio is a function of the integral of the Lorentz transform over the other half of the rotation range, the electron anomalous range.

The equation below for the measured proton/electron mass ratio has two terms, the first term includes mass and the mass equivalent of electrostatic potential energy. The second term removes the electrostatic potential energy of an electron and proton at their closest non-intersecting distance, with the distance adjusted by a function of the ratio v_g/v_m. The second term is also scaled by the integral of the Lorentz factor over the electron anomalous range. The result using only the first term would match the CODATA recommended value to six significant digits, and the result of the full equation matches to ten significant digits[7].

$$\frac{m_p}{m_e} \approx \frac{1}{\left(\dfrac{v_0}{c}\right)^2\left(2\sqrt{\dfrac{\theta_{ea}}{\theta_{L\max}}} - 1\right)} - \frac{E_x\!\left(\left(R_e + R_p\right)\left(1 - \dfrac{\sqrt{2}\sqrt{3}v_g}{v_m}\right)\right)}{\theta_{ea}m_e c^2} \approx 1836.15267353 \tag{36}$$

In the equation above, $E_x()$ represents the equation for the electrostatic potential energy between two charged particles separated by the distance within the parentheses. The electrostatic potential energy equation can be the integral of Coulomb's force equation or its analog given in Equation 33. The subscript x denotes external, meaning that the two particles are separated by at least the sum of their radii. In this case the distance between particles is the sum of their radii, modified by the effect of mass measurement on the electron rest energy. In Equation 24, $\theta_{L\max}$ was shown as the maximum integral of the Lorentz factor with respect to v/c, and the ratio $\theta_{ea}\,/\,\theta_{L\max}$ is analogous to v/c in representing a fraction of the maximum value.

8. Electron *g* factor and charge-photon dynamics

In Section 2, titled 'Electron structure and dynamics', some charge dynamics involved in photon emission were described. In this section additional relevant charge characteristics are described, concluding with the physical basis for the electron *g* factor.

8.1 Integral of |S_r|

Because rotation at v_0 produces the inertial frame of reference of charge, characteristics at v_0 and relative to v_0 are central to charge dynamics. Reference Figure 6 for particle and photon orientation with vector notation. S_r is defined as the special relativistic off-axis component of angular momentum transferred to a photon. As mentioned previously, this component is due to the change in angle that occurs during a charge's change in rotation velocity and the time during which the particles' distance of separation and electrostatic potential energy changes. That |S_r| is equal to $\sqrt{1.25}\,\hbar$ is significant because the integral of the vector magnitude is involved in most physical interactions involving charge, including the relationship expressed by the electron *g* factor.

Defining

$$x \equiv \frac{|S_r|}{\hbar} \tag{37}$$

then

$$\int_0^{\sqrt{1.25}} x\,dx = \frac{5}{8} \tag{38}$$

When $|S_r|$ transitions from 0 to $\sqrt{1.25}\,\hbar$, which occurs during changes of velocity between v_0 and v_1, or v_0 and v_2, the integral of its ratio to $\hbar$ is equal to 5/8. Requisite to this is a frame of reference in which the transition is linear. This integral is equal to the sum of all terms following the kinetic energy term of the Lorentz expansion when rotation is at v_0, as shown in the following.

8.2 Precession at v_0

The MacLaurin series of the Lorentz factor is

$$\gamma = 1 + \frac{1}{2}\frac{v^2}{c^2} + \frac{3}{8}\frac{v^4}{c^4} + \frac{5}{16}\frac{v^6}{c^6} + \dots \tag{39}$$

The series at $v = v_0 = \sqrt{3}/2\,c$ is

$$\gamma_0 = 1 + \frac{1}{2}\frac{\frac{3}{4}c^2}{c^2} + \frac{3}{8}\frac{\frac{9}{16}c^4}{c^4} + \frac{5}{16}\frac{\frac{27}{64}c^6}{c^6} + \dots \tag{40}$$

Since $\gamma_0 = 2$ at v_0 and the second term evaluates to 3/8, the sum of all subsequent terms is 5/8, giving

$$\gamma_0 = 1 + \frac{3}{8} + \frac{5}{8} \tag{41}$$

With regard to rotation and precession, the first term of the series, 1, corresponds to rotation, and all following terms correspond to precession. This is determined from Equation 1, which gives the relationship between precession and rotation as $\omega_p = \omega(\gamma - 1)$. In Equation 41 above, 3/8 corresponds to the kinetic energy term, and 5/8 is the sum of all following terms. The non-kinetic component of precession at v_0 is equal to the integral of $|S_r| / \hbar$ when electron rotation velocity transitions between v_0 and v_1, or v_0 and v_2. This unit-less quantity, 5/8, is one component of charge dynamics involved in photon emission. Those dynamics are seen in the electron g factor given below.

8.3 Electron g factor

The electron g factor is a ratio of the experimentally measured sum of emitted per-axis photon energy including cyclotron emission and anomalous emission to the ratio $(e\,\hbar) / (2m_e)$, where e is the elementary charge. The magnitude of the electron g factor can be formulated as

$$g_e = \frac{2\mu_z}{\frac{e}{m_e}\frac{\hbar}{2}} \approx 2.00231930436146 \tag{42}$$

19

where μ_z is the experimentally determined per-axis electron magnetic moment, and the resultant value given above is based on the experimental result[4] of D. Hanneke et. al.. Within the structural model presented in this article, the theoretical value of g_e shown below is within the standard uncertainty of the experimentally determined value, matching thirteen significant digits.

$$g_e = \frac{\frac{5}{8}\gamma_1}{\theta_{ea}} - \frac{v_g}{c}\frac{2}{\frac{2\pi}{\alpha}+3} \approx 2.00231930436122 \tag{43}$$

9. Planck's constant, quantized energy levels, and galactic rotation velocity

Because they are inextricably interrelated, three equations are presented together. The three equations give 1) quantized energy levels between which proton electron electrostatic potential energy can be emitted. These are often referred to as electron energy "shells", 2) the reduced Planck constant, 3) quantized times between which electron and proton can move together for photon emission.

$$E(n) = \frac{\frac{1}{2}m_e\left(\frac{v_{mp}}{n}\right)^2}{2 - \frac{v_g}{c}\frac{1}{\left(\frac{1}{\frac{5}{8}\gamma_1} - \gamma_1\right)}} \tag{44}$$

$$\hbar = \frac{\frac{m_e}{4}\left(\frac{v_{mp}}{v_m}\right)^2}{\tan\left(\frac{v_{gR}}{c}\right)k_3}\left(1 + \frac{\frac{2\pi}{4}\left(\frac{v_{mp}}{v_m}\right)^4}{\tan\left(\frac{v_{gR}}{c}\right)}\frac{(1+\alpha)}{\left(\frac{1}{\frac{5}{8}\gamma_1} - \gamma_1\right)^{1/2}}\right) \tag{45}$$

$$T(n) = \frac{\left(1 + \frac{\frac{2\pi}{4}\left(\frac{v_{mp}}{v_m}\right)^4}{\tan\left(\frac{v_{gR}}{c}\right)}\frac{(1+\alpha)}{\left(\frac{1}{\frac{5}{8}\gamma_1} - \gamma_1\right)^{1/2}}\right)\left(2 - \frac{v_g}{c}\frac{1}{\left(\frac{1}{\frac{5}{8}\gamma_1} - \gamma_1\right)}\right)}{2\left(\frac{v_m}{n}\right)^2\tan\left(\frac{v_{gR}}{c}\right)k_3} \tag{46}$$

where

$$k_3 \equiv s/m^2 \tag{47}$$

Every photon has an on axis angular momentum of $\hbar$. The units of angular momentum are J s, or Energy Time. The energy a photon carries away is $\hbar/T$, where T is the time over which the photon is emitted. Whatever the photon energy, the product of its energy and its time of emission always equals $\hbar$. Photons can be emitted when proton electron interaction results in a lower electrostatic potential energy. However energy can only be emitted between specific values. The time over which a photon is emitted is constrained to be between certain values. The physical basis of the time constraint is shown in Equation 46. During photon emission the electron's rotation velocity changes from v_2 to v_0, or v_0 to v_1, and the electron and proton move closer together. The change in electrostatic potential energy is transferred to a photon over the time during which the particles move closer together, and the product of the electrostatic energy and time taken for movement is always $\hbar$.

Every variable in the three equations above has been defined. However, that the velocity ratio v_{gR}/c is also an angle with a significant tangent is now introduced. Though v_{gR}/c can be treated as a magnitude in the difference velocity equation relating to v_g, v_{gR} is also a vector. The vector v_{gR} in the solar system is tangential to a line from the galactic center. Rather than distance, the significant relationship is the ratio of tangential velocity to the speed of light. This is represented in Figure 12 below.
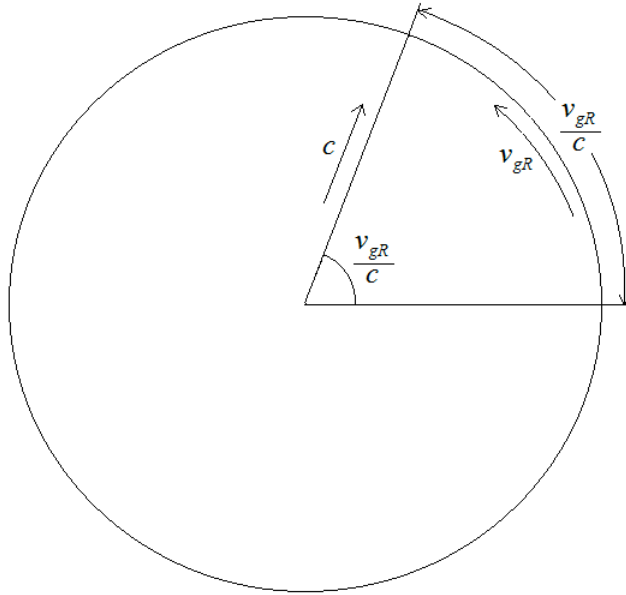

Figure 12: Ratio v_{gR}/c as an arc length and angle

Applying the equation for energy levels to a transition from $n = 2$ to $n = 1$ results in $E(1) - E(2) = 1.63402887773E\text{-}18$ J, or 10.19880615 eV. The CODATA recommended value[7] is 10.19880606 eV for the 2P 1/2 transition. The calculated value differs from the recommended value by a factor of 8.8E-9. This difference is attributable to the effect of time dilation at the earth's surface. While the energy time product $\hbar$ is expected to be constant whether measured at earth's surface or at a location with low gravitational potential, energy measurements alone are affected by a frequency shift of the photon being measured. The Pound-Rebka experiment is an ideal proof of the gravitational potential effect. Equation 44 for energy levels has no adjustment for gravitational potential frequency shift, and so its result would have to be adjusted for the gravitational potential in which measurements are taken.

The result of Equation 45 for the reduced Planck constant, multiplied by 2π, matches the CODATA recommended value of the Planck constant exactly[7]. In this equation, the factor preceding the parenthetical quantity, with $\tan(v_{gR}/c)\,k_3$ as a denominator, if taken alone would give a result matching the recommended value

to five significant digits. Tan(v_{gR} / c) is thus very significant to the constant energy time product, $\hbar$, of every photon. Tan(v_{gR} / c) is also a significant factor in the denominator of Equation 46. Since $E(n) = \hbar$ / $T(n)$, the tan(v_{gR} / c) terms cancel and the equation for energy levels shows no dependency on tan(v_{gR} / c). Because electrons and protons consist of three dimensional rotational motion, and during photon emission they move closer together, along with the rotation and motion of the emitted photon, there are always components of motion in the direction of v_{gR} which are affected by the slope of the angle v_{gR} / c. In these two instances, tan(v_{gR} / c) is associated with the unit transformation k_3.

The other significant component in the denominator of Equation 46 is $(v_m /n)^2$. This component shows the dependence on maximum difference velocity. With $n = 1$, the parenthetical quantity takes its maximum value of v_m. For fractional $n < 1$ to be possible, the parenthetical quantity would have to exceed the maximum, v_m.

Considering quantized energy levels in terms of $E(n) = \hbar\ \omega(n)$, one might expect that $E(n)$ should be factorable into the two components $\hbar$ and $\omega(n)$. However, this is not the case; the terms of $E(n)$ do not factor into the product $\hbar$ and $\omega(n)$ in the sense that the product of two primes can be factored into the two primes. This is because of the cancellation of the tan(v_{gR} / c)k_3 terms in Equations 45 and 46. The significance of this is that energy levels are not independent, but dependent on $\hbar$ and $T(n)$.

The square of the ratio v_m / v_{mp}, the inverse of which appears in Equation 45, has multiple roles. The first role is as proton/electron mass ratio

$$\left(\frac{v_m}{v_{mp}}\right)^2 = \frac{m_p}{m_e} \tag{48}$$

The values of v_{mp} and R_p were determined using the proton/electron mass ratio to satisfy electron and proton angular momentum equations and the kinetic energy component of Equation 9. So Equation 48 is essentially a restatement of the previous solutions. However, the square of the ratio v_m / v_{mp} is also a function of electron mass, the speed of light, and the galactic difference velocity.

$$\left(\frac{v_m}{v_{mp}}\right)^2 = \frac{m_e}{4k_1}\left(c + \frac{5}{8}v_g\right)^4 \tag{49}$$

In Equation 49, unit transformation k_1 is required. But when m_e is replaced with its equivalent representation from Equation 35, the unit transformations cancel, as shown in Equation 50 below.

$$\left(\frac{v_m}{v_{mp}}\right)^2 = \frac{\sqrt{2}\sqrt{3}}{4|v_g||v_m|c^2}\left(c + \frac{5}{8}v_g\right)^4 \tag{50}$$

This cancellation of unit transformations repeats the cancellation of k_1 in the first parenthetical term of Equation 19 when formulated in Equation 32. The value calculated with Equation 50 matches the CODATA recommended value of the proton/electron mass ratio to nine significant digits[7]. What is seen in these equations is a second independent confirmation of the validity of the unit transformation k_1, as well as overall confirmation that mass is an arbitrary designation for effects due to rotation velocities and Thomas precession. The electron's mass, with unit kilogram, is a measure of the effect of velocities as was shown in Equation 35. From Equations 48-50, it is apparent that rather than viewing $(v_m / v_{mp})^2$ as due to m_p /m_e, the mass ratio should be viewed as a description of effects due to $(v_m / v_{mp})^2$. Further, from Equation 50 it can be seen that $(v_m / v_{mp})^2$ and galactic rotation velocity are interrelated.

Rearranging and substituting with Equations 48 and 49, proton mass can be formulated as

$$m_p = \frac{1}{k_1}\left(\frac{1}{2}m_e\left(c + \frac{5}{8}v_g\right)^2\right)^2 \tag{51}$$

The value calculated with Equation 51 matches the CODATA recommended value of the proton mass to nine significant digits[7]. This formulation shows that proton mass has an inverse characteristic relative to electron mass, because in Equation 35 k_1 is in the numerator, and in Equation 51 k_1 is in the denominator. The formulation in Equation 51 also shows that proton mass has a characteristic of the square of electron kinetic energy at a velocity based on v_g. Since v_g is negative, the sum within the inner parentheses of Equation 51 is less than c, and the sum has the characteristic of a difference velocity in being an effective velocity regarding kinetic energy.

It is indicative of structure that in addition to distance between charged particles, their relative orientation contributes to energy levels.

10. Hyperfine transition, or 21 cm emission

Equation 44 for energy levels applies to proton and electron with spins aligned. An additional photon emission is possible with a reversal of the spin orientation between proton and electron. At the $E(1)$ level, the additional emission is called the hyperfine emission, or when referring to photon wavelength, the 21 cm hydrogen spectral line. Because the hyperfine emission occurs at the $E(1)$ level, its energy is a function of the $E(1)$ energy. The equation for the hyperfine emission energy is

$$E_{hf} = E(1) \frac{\dfrac{v_g}{c}\left(\dfrac{v_g}{c}\dfrac{1}{\left(\dfrac{1}{\frac{5}{8}\gamma_1} - \gamma_1\right)} - 1\right)}{\left(1 + \dfrac{\alpha}{2\pi}\right)\left(\dfrac{1}{\left(\dfrac{v_0}{c}\right)^2\left(2\sqrt{\dfrac{\theta_{ea}}{\theta_{L\max}}} - 1\right)} - \dfrac{E_x\left(\dfrac{R_P}{\left(\dfrac{v_0}{c}\right)^4\alpha}\right)}{\theta_{ea}m_ec^2}\right)} \tag{52}$$

E_{hf} calculated using the formula above matches the experimentally determined value[11] to ten significant digits. $E(1)$ is the energy level for $n = 1$. The denominator of the factor on the right is a function of the proton/electron mass ratio, and the numerator of the factor on the right is a function of v_g/c. The primary effect embodied by the equation is a reversal of orientation of particle masses, and the reversal's interaction with v_g/c. To a very rough approximation, $E_{hf} \approx E(1)\,(v_g/c)\,/\,(m_p/m_e)$, and Equation 52 incorporates detailed effects in the same manner as Equations 44 and 36.

Because the proton and electron consist of rotation on three mutually orthogonal axes, interactions on combinations of the axes occur. Instead of a spin-flip on a single axis, or on the vector sum of the three axes, spin-flip can occur on combinations of axes. The three dimensional structure and rotation produces multiple energy sub-levels.

11. Discussion

Briefly summarized in this and the two following paragraphs are the basic theory, model, and experimental results given in preceding sections. The model and proofs presented combine into a consistent overarching view of matter and energy from the particle scale to the galactic scale. The speed of light as a maximum velocity and length contraction solely in the direction of motion lead to angular precession. The difference between rotation and precession gives an effective angular rotation, ω_d, with regard to kinetic energy and angular momentum. The electron and proton, with different radii, different masses, and different maximum difference velocities, have the same maximum angular difference velocity, ω_m, which results in the same per-axis angular momentum, $\hbar/2$. The maximum angular difference velocity, ω_m, also gives electron and proton the same kinetic energy which is an integral component of the electrostatic force formulation in Equation 9. These discoveries required no extension to Thomas precession, and the results of the model and equations match experimental data to eleven significant digits.

The electron's difference velocity at $-v_m$ is balanced with the galactic rotation difference velocity, v_g, with the integral of the Lorentz factor between v_2'/c and v_0/c being central to the balance. Both $-v_m$, and v_g, represent limits. The limiting condition exists when precession on an electrons' axis exceeds rotation by v_m, and the solar system's precession around the galactic center exceeds rotation by v_g. These discoveries required extending Thomas precession to include change in velocity using the integral of the Lorentz factor. The results of the model and equations match experimental data to between ten and thirteen significant digits.

The on-axis angular momentum, or time energy, of a photon is always $\hbar$, and emission of electrostatic potential energy between proton and electron as a photon is constrained to specific values. The constant time energy product, $\hbar$, depends on galactic rotation velocity, v_{gR}. The quantized times between which photons can be emitted also depends on v_{gR}. These cancel to an emitted energy independent of v_{gR}. Also, $(v_{mp}/v_m)^2$ in the equation for $\hbar$ must be multiplied by $(v_m/n)^2$ in the equation for times between which emission can occur, to leave the photon energy a function of v_{mp}^2. These discoveries required extending Thomas precession by recognizing the ratio v_{gR}/c as an angle whose tangent affects photon emission. The results of the model and equations match experimental data to between eight and twelve significant digits.

The theory and models herein are based either directly on Thomas precession, or are logical extensions to Thomas precession. The theory herein is far more than a replacement for a previous theory. The theory herein describes the basis for particle structure, the basis for mass, the physical structural basis for what were previously considered fundamental constants, and the physical structural basis for characteristics such as quantized angular momentum that previously could only be labeled as intrinsic.

Because a point particle approach was used for decades, it is useful in motivating study of the theory and models described herein to briefly discuss some failings of the point particle approach. Beyer et. al. write[12] "[QED] has served as a template for all subsequent quantum field theories. A serious conceptual drawback of this development is not only that our description of nature has become more complicated but also that a parameter was introduced, the dimensionless fine structure constant $\alpha \approx 137$, in order to account for the observed fine structure of hydrogen spectral lines. Since we do not know any way to calculate fundamental constants, such as α, from first principles, the additional constant alpha reduces the predictive power of theory." In contrast with QED, the theory presented herein gives the physical basis for α. Rather than complicating the theory herein, the equations for α give insights that illuminate a single cohesive theory connecting the structure and dynamics of matter from the particle scale to the galactic scale. While α reduces the predictive power of QED, for the model herein α gives deep insights into the electrostatic force.

Beyer gives an interesting perspective into tests of QED which reveal the "proton size puzzle". For example "A recent measurement of the 2S-2P$_{3/2}$ transition frequency in muonic hydrogen is in significant contradiction to the hydrogen data if QED calculations are assumed to be correct." Beyer describes a discrepancy between experimental measurement of proton radius and QED prediction, detailing use of a transition frequency in muonic hydrogen and electron proton scattering experiments. Beyer states "The discrepancy persists and QED is no longer consistent with experimental data".

Because QED predictions deviate from experimental data, it can be said that QED, without predictive power, fails as a theory. Further, if QED served as a template for all subsequent quantum field theories, then those subsequent theories are likewise flawed. A case in point is QCD. In a paper titled "Puzzles in Hadronic Physics and Novel Quantum Chromodynamics Phenomenology", Brodsky et. al. describe[13] "the proton spin problem". The problem involves the fact that "empirically, quarks carry only a small fraction of the proton's spin." Continuing with "The total spin carried by quarks is reduced from the naive 100% down to ≈ 25% of the total spin of the nucleon. This, of course, raises the question of where the remaining 75% comes from." QCD does not explain, and did not predict, the source of 75% of proton angular momentum. In contrast, the theory presented in this article explains proton angular momentum, and also explains why electron and proton have the same angular momentum. A point particle approach has "intrinsic" as the basis for electron $\hbar/2$ per axis angular momentum, and is now searching for a corrective mechanism to QCD to explain proton $\hbar/2$ per axis angular momentum. The theory and model presented herein gives the basis for each particle's angular momentum, and goes further to explain the commonality of $\hbar/2$ to both particles.

QED is not consistent with experimental data describing proton size, and QCD is missing 75% of proton angular momentum. Brodsky et. al. describe an additional seventeen examples "in which experimental results in hadron physics do not agree with conventional expectations." Brodsky et. al. acknowledge "some of these anomalies and puzzles, ... may challenge the assumption that QCD is the correct fundamental theory of the strong and nuclear interactions." Neither Beyer, nor Brodsky describe the purpose of their presentations of experimental and theoretical discrepancies as intended to discredit QED or QCD. However, the number, significance, and scope of the discrepancies dispel any idea that a point particle approach accurately models particle physics or has the predictive power of a viable theory. QED and QCD neither predict the proton radius nor proton angular momentum, and provide no explanation for the common characteristics of proton and electron. If it had none of the aforementioned failings, the point particle approach of the Standard Model (SM) would be too weak to be considered comparable to the theory based on Thomas precession. In the SM, the average mass of the up and down quarks is reported[14] by Patrignani et. al. to be $3.4 ± 0.1$ MeV, given in the MS-bar scheme. Abe et. al. reported[15] the top quark mass as $176 ± 8$(stat.) $± 10$ (sys.) GeV/c^2. The uncertainty of the theoretical calculations, simulations, and measurements is more than 2%. The theory, models, and calculations based on Thomas precession give between eight and thirteen significant digits of correspondence to experimentally determined values, or an uncertainty less than 0.000001%.

In contrast to a point particle approach, the theory and models herein describe particles having structure and rotation calculated from the equation for Thomas precession. This is a physical theory with base units of meters and seconds in a three dimensional space with a relativistic velocity relationship. Accordingly, at a rotation velocity of $\sqrt{3}/2\,c$ precession is equal in magnitude and opposite in direction of rotation, resulting in a frame of reference that meets the operational description of an inertial frame of reference. This inertial frame of reference is significant to the structure of particles and the structure of the Milky Way galaxy.

Some material from previous articles was described again herein both as proof of and background for the latest discoveries. Some material that was not revisited includes further proof of electron and proton radii from neutron and deuteron structure and mass. Additionally, the model of the neutron given in a previous article[3] explains why the neutron has no net charge, but does have magnetic moment and angular momentum. Asymmetrical behavior in orientation or time can be considered consistent with internal structure and inconsistent with a point. Such characteristics include the anomalous photon emission, spin-flip, magnetic moment, and the photon emission time relative to emission period given by the Larmor formula for radiated power of a charge moving through a

magnetic field. Over the last hundred years experimental evidence accumulated for particle structure, and the model based on Thomas precession explains that structure.

The theory and models presented in this and previous articles have applicability in a wide range of scientific disciplines. Because of the breadth of the discoveries, new areas are open for further research. Determining the structure and interaction of particles with galactic rotation in the inner regions of the Milky Way is one topic of interest. Other topics are applying the new understanding to other galaxies and investigating interaction between galaxies. A new hypothesis presented here is that the black hole detected at the center of the Milky Way is an effect of Thomas precession on photon emission at rotation velocity v_0/c. The difference velocity equation, Equation 4, can also be derived from Einstein's relativistic equation for the Doppler effect[3], giving further insights into this topic. Another new hypothesis is that the precession of Mercury's orbit, which is not explained by Newtonian gravitation, is an effect of its orbital velocity interacting with v_g.

On the atomic scale, research remains to generalize the equation relating energy of proton electron orientation at energy level $n = 1$ to all energy levels.

12. Conclusion

Detailed in this article are new discoveries of the role of Thomas precession in the structure of charged particles. Some of the discoveries directly follow from Thomas precession and others follow from Thomas precession extended to incorporate acceleration. The article also describes the discovery that galactic rotation velocity has a balanced interaction with particle rotation. The solar system's observed galactic rotation velocity was proven to be the difference velocity, v_g, with precession greater than rotation. The rest mass and energy of the electron were proven to be functions of v_g and v_m. Electrostatic force and energy were proven to be functions of v_g and v_m. The physical structural basis of quantized energy levels was shown to follow from the quantized time between emissions and the reduced Planck constant. Both quantized time between emissions and Planck's constant were proven to be functions of v_m and v_{gR}. Also the effects of particle orientation were shown, with an equation for the hyperfine emission. The physical structural basis for asymmetry of cyclotron and anomalous emission was shown with difference velocity graphs, and an equation for the electron g factor was given in terms of electron structure.

The physical models of particles, the galaxy, and their interaction have been shown to match experimental data to very high precision. Rapid progress in applying physical structural models based on Thomas precession over the previous year and a half validates the expectations expressed in the first paper on the topic[3]. Because these physical models correctly describe matter and its interactions, new discoveries proceed from previous understanding. The theory and models provide predictive power. Within the next few years, it is expected that full atomic models will enable determining the bases for chemical and material properties. This will enable optimizing material characteristics such as superconductivity, where a point particle approach has failed to explain fundamental properties[16]. The advantages of physical structural models based on Thomas precession are numerous, and high expectations are substantiated by rapid progress.

13. References

1) Einstein A. 1996 [1912], *Einstein's 1912 Manuscript on the Special theory of Relativity*, translated from German by A. Beck, 1996, (2003 ed.), New York, George Braziller, p.58; p.64; p.84; p.100; p.104

2) Smoot, G. F. (1998, February) Physics 139 Relativity Thomas Precession. Retrieved from https://jila.colorado.edu/arey/sites/default/files/files/seven(1).pdf

3) Guynn P. L., viXra [v3] 2017-06-12 15:13:52, 'Electromagnetic Effects and Structure of Particles due to Special Relativity'

4) Hanneke D., Fogwell S., Gabrielse G., Phys. Rev. Lett. 100, 120801 (2008)

5) Nave, R., Hyperphysics Electron Spin Magnetic Moment. Retrieved from http://hyperphysics.phy-astr.gsu.edu/hbase/spin.html

6) Guynn P. L., viXra [v2] 2017-10-07 18:10:32, 'Electrostatic Force and Charge Structure'

7) CODATA Recommended Values of the Fundamental Physical Constants: 2014
J. Phys. Chem. Ref. Data 45, 043102 (2016); doi 10.1063/1.4954402, 57

8) Guynn P. L., viXra [v1] 2017-12-05 19:25:11, 'Proton/Electron Mass Ratio and Gravitational Constant Due to Special Relativity'

9) Palma, Christopher Astro 801 Planets, Stars, Galaxies, and the Universe, 'The Rotation Curve of the Milky Way'. Retrieved from https://www.e-education.psu.edu/astro801/content/l8_p8.html

10) de Grijs, R., Bono G., 2017, Astrophysical Journal Supplement Series 232:22, 'Clustering of Local Group Distances: Publication Bias or Correlated Measurements? V. Galactic Rotation Constants', p. 6

11) Hellwig, H., et. al., 1970, IEEE Transaction on Instrumentation and Measurement, Vol. IM-19, No. 4, 'Measurement of the Unperturbed Hydrogen Hyperfine Transition Frequency'. p.207

12) A Beyer *et al* 2013 *J. Phys.: Conf. Ser.* **467** 012003, 'Precision Spectroscopy of Atomic Hydrogen'

13) S.J.Brodsky, G.deT´eramond and M.Karliner, Ann. Rev. Nucl. Part. Sci. 2012, 62 (2012), 'Puzzles in Hadronic Physics and Novel Quantum Chromodynamics Phenomenology'

14) Abe F., et. al. arXiv:hep-ex/9503002v2 3 Mar 1995. 'Observation of Top Quark Production in *pp* Collisions'

15) C. Patrignani et al.(Particle Data Group), Chin. Phys. C 40, 100001 (2016). 'Quark Masses'

16) Hirsch, J. E., 2009, Physica Scripta Vol 80, No. 3, 'BCS theory of superconductivity: it is time to question its validity'